Enhancement of high-order harmonic generation in the presence of noise



2011 J. Phys. B: At. Mol. Opt. Phys. 44 135403

(http://iopscience.iop.org/0953-4075/44/13/135403)

J. Phys. B: At. Mol. Opt. Phys. **44** (2011) 135403 (9pp) doi:10.1088/0953-4075/44/13/135403

# Enhancement of high-order harmonic generation in the presence of noise

**I Yavuz[1], Z Altun[1] and T Topcu[2]**

[1] Department of Physics, Marmara University, 34722 Ziverbey, Istanbul, Turkey
[2] Department of Physics, Auburn University, AL 36849-5311, USA

E-mail: ilhan.yavuz@marmara.edu.tr

Received 14 February 2011, in final form 28 April 2011
Published 17 June 2011
Online at stacks.iop.org/JPhysB/44/135403

**Abstract**
We report on our simulations of the generation of high-order harmonics from atoms driven by an intense femtosecond laser field in the presence of noise. We numerically solve the non-perturbative stochastic time-dependent Schrödinger equation and observe how varying noise levels affect the frequency components of the high harmonic spectrum. Our calculations show that when an optimum amount of noise is present in the driving laser field, roughly a factor of 45 net enhancement can be achieved in high-order harmonic yield, especially, around the cut-off region. We observe that, for a relatively weak noise, the enhancement mechanism is sensitive to the carrier-envelope phase. We also investigate the possibility of generating ultra-short intense attosecond pulses by combining the laser field and noise and observe that a roughly four orders of magnitude enhanced isolated attosecond burst can be generated.

(Some figures in this article are in colour only in the electronic version)

## 1. Introduction

High-order harmonic generation (HHG) has been a very hot research topic over the last couple of decades due to its potential applications for generating radiation sources whose energies cover a range from the vacuum ultraviolet to soft x-ray region. It has become a major resource in generating attosecond pulses [1] and also revealed some revolutionary applications and ideas, such as real-time probing of chemical reactions [2] and high resolution tomographic orbital imaging [3]. The HHG process can be described by a semi-classical three-step model [4], in which an electron first tunnels through an atomic potential barrier suppressed by a driving laser field and ends up in the continuum with zero kinetic energy. The subsequent motion of the electron in the laser field is treated classically. The electrons in the continuum are accelerated first away from and then towards the parent ion under the action of Coulomb attraction and the laser field, gaining kinetic energy. The electrons which are driven back close to the core can either be scattered or else recombined with the atom core, emitting a burst of photons as the system returns to the ground state. The photons can have energies up to $I_p + 3.17U_p$, where $U_p = E_0^2/4\omega_0^2$ is the ponderomotive potential and $I_p$ is the ionization potential. Photon frequencies in multiples of fundamental laser frequency ranging from 1 up to 300 have been reported [5].

There have been intense efforts to increase conversion efficiency for producing high harmonics to the level needed in applications, such as nanoscale lithography and holography. In optimization studies, close attention has been given to the parameters of the driving laser pulse such as the pulse shape, carrier-envelope phase (CEP) and chirp [6], and macroscopic parameters such as target gas pressure, size of the medium and focus position [7]. The major purposes of the optimization efforts are to extend the plateau region and to obtain high intensity harmonics. Combining different colour pulses [8, 9] and different species of gas targets [10], it has been demonstrated that several orders of magnitude enhancements can be achieved. While optimization of the macroscopic parameters is intended to achieve the best phase matching of the generated harmonics, tweaking of the laser parameters aims to increase ionization with *minimal depletion* of the atomic ground state. The ionization that initiates the three-step HHG process mostly happens through tunnelling, which by restricting the kinetic energy of the electrons permits them to recombine with their parent ion. The limited kinetic energy minimizes the number of atoms which are completely ionized and thus unable to contribute to HHG. This is also one of

 

the main reasons why the semiclassical three-step model has been so successful in simulating the high harmonics since this model assumes that electron tunnel ionizes into continuum with zero kinetic energy and can be turned around by the laser field to recombine before it escapes. As a result of this, there is a limit as to how high in intensity one can go before the three-step model starts to deviate substantially from experimental observations. Classical simulations have shown that if the ionized electron does not return to its parent ion and recombine typically within the first few half cycles of the driving laser, chances are that it will escape. Therefore, in order to enhance the intensities of the high harmonics generated, it is not necessarily useful by itself to enhance the total ionization rate, but rather to enhance the ionization rate dominated by the electrons which have low kinetic energy immediately upon ionization and can therefore contribute to harmonic generation.

A rather non-intuitive way to increase the ionization rate is through what is called a stochastic resonance [11]. It manifests itself as an enhanced signal-to-noise ratio in a physical system periodically driven by a weak laser field coupled with a stochastic field. The dynamical process behind this resonance phenomenon can be attributed to virtual transitions caused by the noise field between non-resonant states which may facilitate ionization. A time domain description of a stochastic resonance can also be given in terms of matching of inherent time scales induced in a physical system [11]. These time scales for our problem are the period of the driving laser and the average time between random occurrences of transitions caused by the stochastic noise field within a laser period. Matching of these two time scales can be looked upon as a stochastic resonance condition, and has been observed in a wide range of physical systems. For instance, classical and quantum mechanical simulations have shown enhanced chaotic ionization and excitation of Rydberg atoms in microwaves superposed with noise [12]. Manifestations of this type of resonance have been revealed in simulations of photoionization of atoms [13, 14] and photodissociation of molecules [15] by intense femtosecond laser pulses as enhanced total ionization and photodissociation probabilities. In [13], Singh *et al* report that by adding Gaussian white noise to a femtosecond infrared (IR) pulse, it is possible to enhance the total ionization probability by a factor of $\sim$30 in a hydrogen atom. Although the total ionization probability displays such an increase due to the emergence of a stochastic resonance, it is not obvious to us whether this would result in an increase in the intensity of the high harmonics which can be generated in such a stochastic field, or if it would, how much enhancement it would yield. The question becomes exactly how much of the total increase in the flux of the ionized electrons resulting from an induced stochastic resonance is due to the increase in the ionization that actually contributes to the HHG process and not simply attributable to direct ionization.

From an experimental point of view, the use of chaotic light rather than Gaussian white noise has advantages. As Singh *et al* point out in [13], it can be generated by superposing a wide band of frequencies with random phases [16], which can be substituted for Gaussian white noise as they do in their work. The difficulty in our case, however, is the requirement for high intensities needed for high harmonic generation. Although noise at such high intensities has not really been experimentally realized to our knowledge, one way we can envision the possibility of producing it would be to generate the combined laser–noise field rather than laser and noise fields separately, in order to combine them later. It is well known that spatial and temporal characteristics of strong laser pulses can be manipulated by propagating them through macroscopic media, particularly optical fibres [17, 18]. Such manipulations are typically employed spatio-temporally engineered light pulses. We suspect that it may be possible to propagate a strong laser pulse through a specially designed optical fibre whose crystal structure contains imperfections, such as dislocations, vacancies or interstitials, in order to distort its temporal profile. This may distort the laser pulse as it scatters at these random centres (imperfections) during its propagation through the optical fibre. If it is feasible, the advantage of this approach would be that it would make the necessity to generate a separate strong noise field obsolete since the stochastic character would get sculpted into the spatio-temporal profile of the pulse as it propagates. The effective intensity of the noise, which comes from the random scatterings of the laser pulse itself, would be commensurate to that of the fundamental laser pulse itself.

Our main goal in this study is to demonstrate that the stochastic ionization mechanism explored in [13] does result in enhanced HHG yield, using $He^+$ as an example. The specific emphasis here is given to the dependence of the total ionization probability on the noise amplitude, the power spectrum and its dependence on the CEP, and the enhancement of the HHG yield as a function of noise amplitude. We also investigate the generation of isolated attosecond pulses in the presence of noise. The paper is organized as follows. Section 2 outlines the theoretical method used to simulate the interaction of $He^+$ ions with the laser field coupled with a stochastic field within a one-dimensional model involving the propagation of the time-dependent Schrödinger equation (TDSE). The details of the numerical method used in solving the time-dependent wave equation are briefly described in this section. Section 3 presents the dependence of the ionization probability on the noise amplitude, the power spectrum with and without noise, and net enhancement factors for HHG yield. Section 4 presents results for attosecond pulse generation from harmonics belonging to a broad plateau spectrum obtained in the presence of noise. Finally, we summarize our results in section 5.

## 2. Theoretical method

The interaction of an atom with a linearly polarized intense laser field can be modelled via a one-dimensional TDSE within the single-active electron approximation. The TDSE gains a stochastic character by the addition of noise to the interaction potential. In order to model the interaction of a single atom with a stochastic laser field, we solve the one-dimensional TDSE in the length gauge with a model

potential representing the one-dimensional Coulomb attraction in Cartesian coordinates:

$$\mathrm{i}\frac{\partial\psi(x,t)}{\partial t} = \left[-\frac{1}{2}\frac{\partial^2}{\partial x^2} - \frac{2}{\sqrt{x^2+a}} - xE(t)\right]\psi(x,t), \qquad (1)$$

where the value of the parameter $a$ is set to 0.5 au so as to produce the ground state eigenenergy of $-2.0$ au of the $He^+$ ion. Atomic units are used throughout this paper unless we explicitly state otherwise. The stochastic electric field represented by $E(t)$ is assumed to have the following explicit form:

$$E(t) = E_0 f(t)\sin(\omega_0 t + \phi) + N(t), \qquad (2)$$

where $E_0$ and $\omega_0$ are the laser field amplitude and the fundamental frequency of the driving laser, respectively. $\phi$ is the CEP and $N(t)$ represents the additional noise field. In all our simulations, we use white noise with a zero mean uniform amplitude distribution, $\langle N(t)\rangle = 0$, with an effective amplitude $\kappa$ which has the statistical property that $\langle N(t)N(t')\rangle = 2\kappa^2\delta(t-t')$. In order to take average of the physical quantities over an ensemble of a sufficient number of stochastic realizations, the simulations were repeated 100 times for each noise amplitude.

The pulse envelope denoted by $f(t)$ is assumed to have a sine-squared shape:

$$f(t) = \begin{cases} 0 & t \leqslant 0 \\ \sin^2(\pi t/T_p) & 0 < t < T_p \\ 0 & t \geqslant T_p, \end{cases} \qquad (3)$$

where $T_p$ is the pulse duration. In this study, we used a laser field with a fundamental wavelength of 800 nm ($\omega_0 = 0.057$ au). The interacting laser pulse exhibits four-cycles which lasts for about 10.8 fs. With these choices of parameters for the laser field together with the ionization potential of the $He^+$ ion, the Keldysh parameter $\gamma$ satisfies $\gamma < 1$, suggesting that the ionization dynamics predominantly falls into the tunnelling regime.

For the numerical solution of equation (1), the box size was chosen to be 800 au, where the spatial variable $x$ runs between $-400$ and 400 au, with a grid spacing of 0.2 atomic units. The time step is 1/4096 of an optical cycle, which is small enough to give converged results. A smooth mask function which varies from 1 to 0 starting from half way between the origin and the box boundaries on both sides is multiplied with the solution of equation (1) at every time step to avoid spurious reflections from the box boundaries. When the time-dependent solutions are obtained at each time step, they are then used to calculate the time-dependent ionization probability

$$P(t) = 1 - \int |\psi(x,t)|^2\,\mathrm{d}x. \qquad (4)$$

In order to evaluate the total ionization probability resulting from the pulse, we propagate the wavefunction long enough after the pulse is over until the time-dependent ionization probability converges.

The photon-emission probability of an atom is proportional to the Fourier transform of the acceleration form of the dipole interaction, $a(\omega)$, between the active electron and the applied laser field. We obtain the dipole acceleration in time domain $a(t)$ and its Fourier transform $a(\omega)$ through

$$a(t) = -\langle\psi(x,t)|[H,[H,x]]|\psi(x,t)\rangle \qquad (5)$$

$$a(\omega) = \int a(t)\,\mathrm{e}^{-\mathrm{i}\omega t}\,\mathrm{d}t. \qquad (6)$$

The spectral density of the radiation emitted for the entire time, i.e. the power spectrum, is proportional to $|a(\omega)|^2$, which we refer to as HHG yield, $I$.

We monitor the enhancement in the high harmonic yield due to the presence of noise as a function of noise amplitude by surveilling $|a(\omega)|^2$. In addition to monitoring individual harmonics, we found that it is also beneficial to monitor collective enhancement in the HHG plateau by integrating $|a(\omega)|^2$ over a range of harmonics and treat this as a measure of enhancement. The integrated $|a(\omega)|^2$ between harmonics with frequencies $\omega_i$ and $\omega_f$ is

$$I = \frac{1}{3c^3}\int_{\omega_i}^{\omega_f} |a(\omega)|^2\,\mathrm{d}\omega. \qquad (7)$$

As an aid to quantitatively monitoring enhancement, we define a numerical enhancement factor $\eta$,

$$\eta = \frac{I(L+N)}{I(L)+I(N)} - 1, \qquad (8)$$

where $I(L)$ and $I(L+N)$ are the integrated HHG yields calculated in the absence and in the presence of noise, respectively. $I(N)$ is the integrated HHG yield calculated in the presence of noise alone. The above expression is adapted from the formula used to monitor the net enhancement in the atomic ionization probability by Singh *et al* [13]. The only difference is the replacement of ionization probabilities with integrated HHG yield within a range of harmonics characterized by the frequencies $\omega_i$ and $\omega_f$. It should be noted that the enhancement in the integrated HHG yield goes to zero when either of the $I(L) \gg I(N)$ or $I(L) \ll I(N)$ inequalities hold. In other words, the net enhancement goes to zero when either the laser pulse or the noise field substantially dominates. Depending on whether the HHG yield of an individual harmonic or a range of integrated harmonics is used, the enhancement factor $\eta$ delegates enhancement in either a given harmonic or a portion of the plateau region in the HHG spectrum. We resort to both approaches below.

## 3. Enhancement of ionization and HHG yield under noise

We begin by discussing our simulations for the ionization of a $He^+$ ion interacting with a laser field alone with zero CEP. The laser pulse is assumed to have a peak intensity of $1.0 \times 10^{15}$ W cm$^{-2}$ with a duration of four-cycles and wavelength of 800 nm. Once the time-dependent wavefunction is calculated at each time step, equation (4) is used to calculate the ionization probability.

Figure 1 shows the change in the total ionization probability as a function of time for three different cases. The

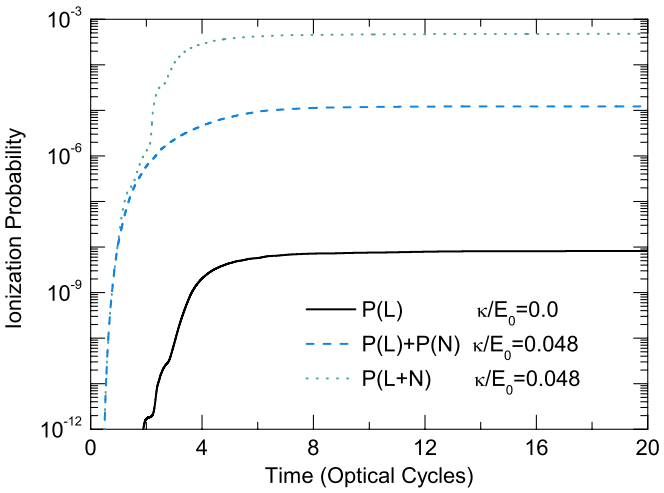


**Figure 1.** The variation of the time-dependent ionization probability of the $He^+$ ion for two different noise amplitudes in a 4-cycle, 800 nm laser field with a peak intensity of $1.0 \times 10^{15}$ W cm$^{-2}$ and $\phi = 0$. The laser field and noise is turned off after 4-cycles. The solid (black) curve represents the results from the laser field alone, the dashed (blue) curve represents the results from the simple sum of the laser field alone and noise alone, and the dotted (green) curve displays the results obtained by including noise and the laser field. The ionization probabilities in the presence of noise are averaged over 100 different realizations.

solid (black) curve labelled as $P(L)$ represents the ionization probability for the $He^+$ ion interacting only with the laser field. The dashed (blue) curve labelled as $P(L) + P(N)$ represents the simple sum of the ionization probabilities $P(L)$ and $P(N)$, the latter being the ionization probability in the presence of noise alone. The dotted (green) curve labelled as $P(L + N)$ is the ionization probability for the case in which the laser field and noise are applied simultaneously. The amplitude of the noise used in the simulations of figure 1 is chosen to correspond to a noise-to-laser amplitude ratio of 0.048. As can be seen from the curve labelled as $P(L)$ in figure 1, the ionization probability increases during the laser pulse and saturates to a small value of $\sim 10^{-8}$ by the end of the laser pulse. The curve labelled as $P(L) + P(N)$ is plotted as a reference to see how much ionization is caused by the two separate fields of the IR laser and noise individually, excluding any enhancement in ionization that may arise from the formation of a stochastic resonance. $P(L) + P(N)$ saturates to a value of $\sim 3 \times 10^{-5}$, which is roughly three orders of magnitude larger than the value attained by $P(L)$. This increase in the ionization probability solely comes from the applied noise field *alone*.

The addition of noise to the driving laser field changes the ionization probability $P(L + N)$ drastically. The ionization probability rapidly increases to its saturation value $\sim 4 \times 10^{-4}$, which is well over four orders of magnitude larger than that of $P(L)$. The drastic increase in the ionization probability attained by the addition of noise can only be attributed to the formation of a stochastic resonance since neither laser nor noise alone can account for this increase by themselves, as suggested by the sum of the separate ionization probabilities, $P(L) + P(N)$. According to Singh *et al* [13], in the simultaneous application of the laser field and noise, non-resonant excitations play a central role in the enhancement mechanism. In other words, virtual transitions are caused by the noise field between non-resonant states, which can facilitate ionization. In an alternative picture in time domain, the existence of a stochastic resonance can be attributed to the approximate matching of two different time scales inherent in the combined laser–noise–atom system [11]. The first time scale is set by the driving laser and is the period of the laser field. The second time scale arises from the interaction of the atom with the stochastic field. It is important to note here that there is no inherent time scale associated with the noise field itself. Rather, this time scale is a property of the combined noise–atom system. In order to get this time domain picture, it is sufficient to consider two identical atoms driven by two noise fields with field strengths $\kappa_1$ and $\kappa_2$, such that $\kappa_1 \leqslant \kappa_2$ and $\kappa_1$ is small but still able to induce transitions between virtual bound states. The impulsive kicks delivered to the bound electron by the noise field happen at random intervals, but some are actually strong enough to cause transitions. The larger $\kappa_2$ would then also drive transitions (or even ionization if large enough), but the average number of impulsive kicks received by the electron per unit time, which are strong enough to cause transitions, would be larger compared to the weaker driven case. In other words, there are simply more occurrences of impulsive kicks in unit time interval for the noise field with $\kappa_2$ that is strong enough to cause transitions. If we take a unit time to be the laser period, then the average number of hoppings between the virtual states caused by the noise field per laser period would define an average frequency. It is the matching of this average frequency and the frequency of the laser field that creates a resonance condition.

The average time between occurrences of noise-induced virtual transitions approximately matches the laser period for the modest noise-to-laser amplitude ratio ($\kappa/E_0 = 0.048$) in figure 1, resulting in roughly a four orders of magnitude increase in the total ionization probability. The ionization probability $P(L + N)$ in figure 1 starts dominating the ionization probability $P(L) + P(N)$ after the driving laser field amplitude becomes high enough to effectively introduce another time scale into the dynamics. This is the average time between noise-induced hoppings between the virtual states dressed by the laser field. When the average time between these hoppings amongst non-resonant states are matched by the period of the driving laser field, the stochastic resonance condition is satisfied.

In figure 2, we plot the converged ionization probabilities after the laser pulse is turned off as a function of the ratio of the noise amplitude $\kappa$ to the laser field amplitude $E_0$. The (green) solid curve with open squares represents the ionization probabilities when only the noise field is applied ($P_C(N)$), the (black) dashed curve with open circles shows the ionization probabilities from the combined laser–noise field ($P_C(L+N)$), and the (blue) dotted curve with open triangles shows the simple sum of the ionization probabilities ($P_C(L) + P_C(N)$) from separate applications of the laser field and noise. The ionization probability when only the laser field is applied is depicted as the horizontal dashed line labelled as $P_C(L)$.

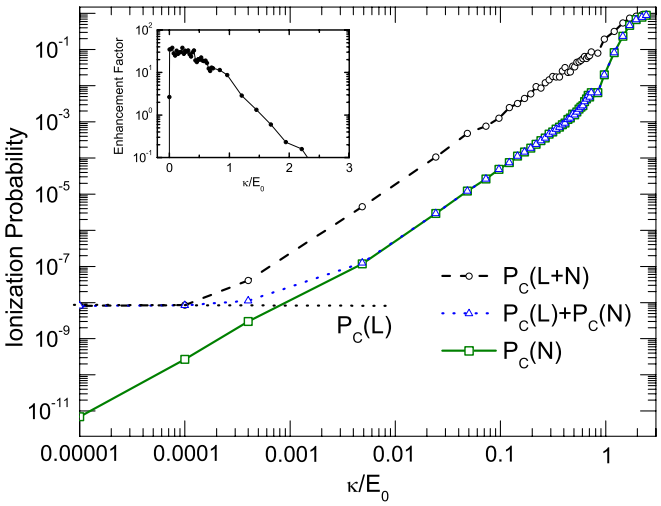


**Figure 2.** Noise amplitude dependence of the converged ionization probability for the $He^+$ ion calculated for fixed laser intensity. The laser field parameters are the same as those in figure 1. The horizontal axis is scaled to a laser field amplitude (0.169 au) and the ionization probabilities are averaged over 100 different realizations. The data points are the results of individual calculations (a) when laser field and noise are introduced simultaneously (dashed (black) curve with open circles), (b) when only the noise is applied (solid (green) curve with open squares) and (c) the sum of the converged ionization probability of the laser alone and the noise alone at each noise amplitude (dotted blue curve with open triangles). Note that the ionization probability converges to $9.0 \times 10^{-9}$ when $\kappa = 0$. The inset shows the net enhancement in the ionization probability as a function of a noise-to-laser ratio.

When the simple sum of the separate ionization probabilities $P_C(L) + P_C(N)$ is compared with the ionization probabilities $P_C(L + N)$ arising from the simultaneous application of the laser field and noise, it is clear that a substantial increase in the ionization is induced for $\kappa/E_0 > 0.001$ all of the way up to $\kappa/E_0 \sim 1$. Well over an order of magnitude enhancement in the ionization probability is achieved for $\kappa/E_0 > 0.01$. The case presented in figure 1 falls in this range ($\kappa/E_0 > 0.048$).

Note that the ionization probability in the combined laser–noise field converges to the ionization probability of the laser field alone when the noise amplitude vanishes as expected. In the opposite limit where the noise amplitude becomes comparable to that of the driving laser field, the total ionization probability is essentially due to the noise field alone. In either of these extreme limits, i.e. when the driving field is either dominated by the laser field or the noise alone, the ionization comes from the dominating field, and we cannot speak of the stochastic resonance condition. In other words, in either of these limits, the net enhancement factor for the ionization probability, $[P_C(L + N)/(P_C(L) + P_C(N))] - 1$, vanishes. This can be seen from the inset in figure 2. The sharp rise in the net enhancement factor right around zero is followed by a relatively broad maximum until the noise-to-laser amplitude ratio becomes unity. It then starts decreasing quite rapidly to zero until the noise-to-laser amplitude ratio becomes about 2.2. This would be the regime in which the average frequency of hoppings between the virtual states caused by the noise field is much higher than the frequency of the driving laser field and the stochastic resonance condition is no longer satisfied. It is interesting to note that the noise with an amplitude equal to about 1/10 of the amplitude of the driving laser field suffices for the optimum enhancement. The broad maximum in the net enhancement is clearly reflected in the relatively sharp increase in the ionization probabilities as can be easily seen in the associated curves in figure 2. The interesting regime, in which the net enhancement factor of the ionization probability is large, corresponds to the range $0.01 < \kappa/E_0 < 0.5$, and this would be the dynamical regime where two different time scales in the dynamics, i.e. the laser period and the average time between the occurrences of noise-induced transitions per laser period, approximately match.

The harmonic spectra of a $He^+$ ion calculated in the presence of a laser field alone can be seen as the solid black curves in figures 3(a) and (b), corresponding to CEPs $\phi = 0$ and $\phi = \pi/2$, respectively. The harmonic spectra calculated in the combined laser–noise field with the same CEPs are also plotted in the same figures by the red and green solid curves. The contribution to the HHG process results from both short and long quantum trajectories, depending on the ionization time of the active electron. The spectrum in the plateau region exhibits a complicated interference structure rather than isolated harmonics separated by twice the driving laser field frequency. Each harmonic is formed upon the recombination of an ionized electron with its parent ion following different quantum paths. These degenerate quantum trajectories lead to different time-dependent dipole phases in the dipole moment, which creates irregular substructures within each harmonic. Figure 3(a) shows that the harmonic spectra generated in the combined laser–noise field exhibit dramatically enhanced harmonics in intensity compared to the spectrum obtained in the laser field alone. The spectra calculated in the combined laser–noise fields are noticeably smoother than the ones calculated in the laser field alone and this is mainly the result of averaging over many realizations of the HHG spectra corresponding to many realizations of the stochastic field. The total ionization probability corresponding to the field intensity and the noise amplitude used for the red curve ($\kappa/E_0 = 0.097$) in figure 3(a) is $\sim 10^{-3}$. The ionization probability for the laser–noise parameters used in generating the green curve ($\kappa/E_0 = 0.194$) is higher, but falls into the same range of the net enhancement factor from figure 2, which is why the red and the green spectra are so similar in both figures 3(a) and (b). Simply comparing the black spectra calculated in the laser field alone to either of the green or red spectra in figure 3 suggests an eight orders of magnitude enhancement in the high-harmonic intensities, whereas roughly a five orders of magnitude enhancement in the total ionization probability was observed from figure 2. This confirms our suspicions that enhancement in the total ionization probability does not linearly translate into harmonic intensities, or to put it more precisely, harmonic generation is not enhanced commensurately with the increasing total ionization probability resulting from the induced stochastic resonance.

The harmonic spectrum in the presence of the laser field alone corresponding to $\phi = 0$ shows a visible difference

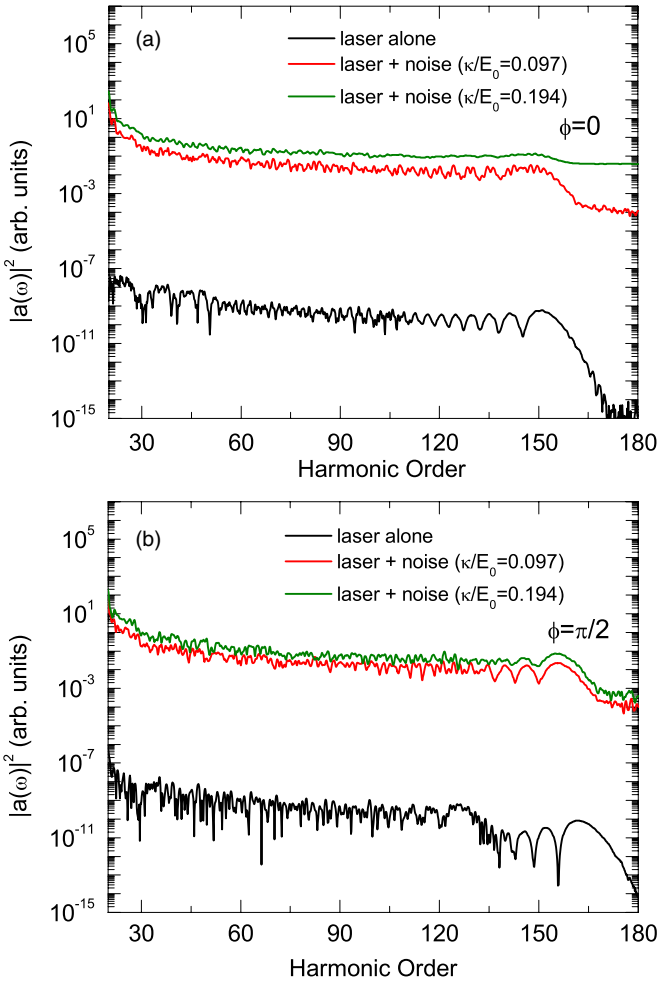


**Figure 3.** High harmonic spectrum for $He^+$ for the same laser field parameters as used in figure 1, for two different CEPs. The black curve represents the HHG spectrum in the presence of the laser field alone, and the red and green curves represent the spectra in the combined laser field and noise driving with $\kappa/E_0 = 0.097$ and $\kappa/E_0 = 0.194$. In the case of the red curve ($\kappa/E_0 = 0.097$), the laser field amplitude is roughly ten times larger than that of the noise, and results in a factor of $\sim 9 \times 10^4$ increase in the total ionization probability. The increase in the total ionization probability for $\kappa/E_0 = 0.194$ is roughly by a factor of $\sim 7 \times 10^5$ when compared to that of the laser field alone.

around its cut-off region from that of corresponding to $\phi = \pi/2$. The temporal profile of the driving laser field with $\phi = \pi/2$ allows two cut-offs and this is the main reason for the difference. It should be noted that a longer pulse with a larger number of cycles under the carrier field envelope would undoubtedly display a much less significant effect attributable to CEP. The addition of noise dramatically increases the intensity of the stochastically averaged power spectrum independent of the choice of CEP for the driving laser field, as can be seen by comparing figures 3(a) and (b). The dependence of net enhancement factors on the noise amplitude for a fixed peak laser field amplitude, $E_0$, is investigated for several individual harmonics and results are tabulated in table 1 for two different CEP values. The ratio between the net enhancement factors corresponding to $\phi = 0$ and $\phi = \pi/2$ gradually increases as a function of an increasing noise-to-laser ratio and becomes roughly unity by the time when the noise amplitude becomes roughly 30% of the fixed peak laser field amplitude.

**Table 1.** Net enhancement factors for different CEPs and the $\kappa/E_0$ ratio for some selected harmonics, represented as $q$, where $\kappa$ and $E_0$ are the noise and laser field amplitudes, respectively. The laser field parameters are set the same as in figure 1 and the factors are averaged over 100 realizations.

| | $\phi = 0$ $\kappa/E_0$ | | | | $\phi = \pi/2$ $\kappa/E_0$ | | | |
|---|---|---|---|---|---|---|---|---|
| $q$ | 0.005 | 0.097 | 0.194 | 0.313 | 0.005 | 0.097 | 0.194 | 0.313 |
| 135 | 8 | 43 | 37 | 30 | 13 | 36 | 38 | 27 |
| 137 | 7 | 21 | 71 | 45 | 2 | 7 | 32 | 30 |
| 139 | 10 | 20 | 26 | 47 | 30 | 42 | 27 | 35 |
| 145 | 11 | 67 | 84 | 75 | 9 | 51 | 34 | 45 |
| 149 | 12 | 84 | 99 | 60 | 1 | 20 | 55 | 24 |

Another feature in figure 3 to notice is that the HHG spectra calculated using a combined laser–noise field are substantially smoother than their counterparts calculated in a laser field alone. Computationally, this is due to the statistical averaging of different realizations of the combined laser–noise field. A somewhat similar smoothening effect also emerges when high harmonics are propagated through a macroscopic medium [19]. The propagation of high harmonics generated in a macroscopic medium cleans and resolves single atom harmonic spectra into either odd or even harmonics, generating experimentally observed spectra. The main propagation mechanism in this sense can be modelled solving Maxwell's equations in which the single atom spectra would serve as a source term. What Maxwell equations essentially do is that they add up the source term as the generated harmonic fields propagate through the medium. This is in a way similar to averaging over an ensemble of laser fields within a range of laser intensities due to the localized spatial profile of a focused laser pulse. Therefore, we expect that the same *smoothening* effect as we see in figure 3 would be inherited when the generated high harmonics are propagated through a macroscopic medium since the spectra averaged over different realizations of the stochastic laser–noise field would become the source term in Maxwell's equations.

The integrated HHG yield is calculated as a function of the same noise-to-laser ratio used in figure 2 for three different cases using equation (7) with $\omega_i = 120\omega_0$ and $\omega_f = 170\omega_0$ integration limits and the corresponding results are depicted in figure 4. Note that the integration limits straddle the cut-off region. The dotted-truncated horizontal line labelled as $I(L)$ represents the integrated HHG yield from the laser alone; the dotted (red) curve with open triangles labelled as $I(L) + I(N)$ represents the sum of the harmonic yields calculated separately for the laser field alone and noise alone; solid (black) curve with open squares labelled as $I(L + N)$ represents the integrated HHG yield obtained by the simultaneous application of noise and laser fields. The inset in figure 4 is the net enhancement in the integrated HHG yield due to the addition of the noise calculated with equation (8). The integrated HHG yield represented by

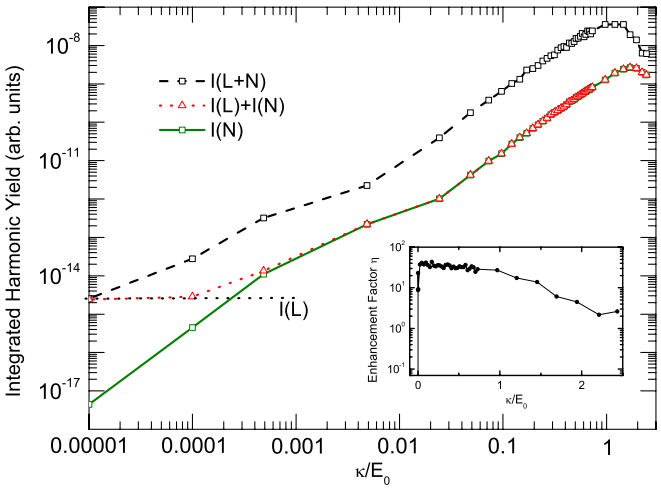


**Figure 4.** The variation of the integrated HHG yield as a function of the noise amplitude for a fixed laser field intensity of $1.0 \times 10^{15}$ W cm$^{-2}$. The laser field parameters are the same as those in figure 1. The values are averaged over 100 realizations. $I(L)$ represents the harmonic yield from the laser alone, the dotted (red) curve with open triangles labelled as $I(L) + I(N)$ represents the harmonic yield obtained from the sum of the separate laser field alone and noise alone calculations, and solid (black) curve with open squares labelled as $I(L + N)$ represents the results obtained from the combined laser–noise field. The inset is the net enhancement in the harmonic yield due to noise addition calculated with equation (8).

$I(L) + I(N)$ and $I(L + N)$ gradually rises to a maximum, then they start decreasing as the stochastic effects become dominant when the noise amplitude becomes larger than that of the driving laser field. The reflection of this behaviour is also visible in the net enhancement factor calculated from equation (8) and shown in the inset in figure 4. The inset clearly shows the tendency of the net enhancement in the integrated HHG yield to decrease as a function of an increasing noise-to-laser ratio. It is interesting to note that the net enhancement for the lower limit of noise-to-laser ratio quickly deviates from zero and increases very sharply. Any value of the noise-to-laser ratio within the $5 \times 10^{-4} < \kappa/E_0 \leqslant 1$ range seems sufficient to gain a relatively high net enhancement in the integrated HHG yield, as indicated by the inset in figure 4. As soon as the noise becomes dominant the net enhancement begins to decrease as expected.

The non-monotonic resonance-like behaviour in the net enhancement factor depicted in the inset in figure 4 may be attributed to the stochastic resonance phenomenon resulting from the constructive role of noise in the ionization process. A similar behaviour in the enhancement of photoionization of a hydrogen atom in the presence of the laser field and noise was observed by Singh *et al* [13]. The broad peak in the net enhancement curves in the inset in figure 4 suggests a range of noise amplitudes which can be useful in achieving enhancement. The dependence of net enhancement factors on noise amplitude for a fixed peak laser field amplitude are tabulated in table 2 for two different CEP values. Again, the ratio between the net enhancement factors corresponding to two different CEPs gradually increases with an increasing noise-to-laser ratio and becomes unity when $\kappa/E_0$ is roughly $1/3$.

**Table 2.** Net enhancement factors $\eta$ in the integrated HHG yield for different CEPs and the $\kappa/E_0$ ratio, where $\kappa$ and $E_0$ are the noise and laser field amplitudes, respectively. The laser field parameters are set the same as in figure 1 and the $\eta$ values are averaged over 100 realizations.

| | $\phi = 0$ | | | | $\phi = \pi/2$ | | | |
|---|---|---|---|---|---|---|---|---|
| $\kappa/E_0$ | 0.005 | 0.097 | 0.194 | 0.313 | 0.005 | 0.097 | 0.194 | 0.313 |
| | 8 | 42 | 35 | 31 | 5 | 25 | 30 | 30 |

The time-dependent evolution of the probability density corresponding to the wavefunction of the system is seen in figure 5 for the noise and laser field parameters used in figure 1. The black curve is for the case in which only the laser field is present, and the grey curve is for the case when the combined laser–noise field is applied. Recalling that the interaction time is four-cycles, zero and 12-cycle snapshots in figure 5 show the probability distribution in space before and well after the laser pulse (and noise) is turned off. The time evolution between these two snapshots shows the differences in both the amplitude and the structure of the laser alone and combined laser–noise driven cases. In the combined laser–noise field, the amplitude of the outgoing and returning parts of the wavefunction have substantially larger amplitude compared to the laser driven case alone, accounting for the enhanced ionization and recombination through the induced stochastic resonance. The wavefunctions for the combined laser–noise driven case also show many irregular structures compared to the laser driven case, which we attribute to the ionization aided by the hopping of the electron between the non-resonant states due to the action of the simultaneously applied noise.

## 4. Attosecond pulse generation in the presence of noise

When the laser pulse duration is as short as a few optical cycles, it becomes considerably harder to spectrally resolve the harmonics in the plateau region due to the blue-shifting in the peak positions of the harmonics. The interference between different quantum paths of the returning electron causes splittings in the spectral profile of a given harmonic, which complicates its identification. The high harmonic generation obtained from few cycle laser pulses is considered to be the best method to generate ultra-short attosecond pulse trains or single isolated attosecond pulses [20, 21]. The main approach for synthesizing an attosecond pulse from high harmonics is to use a range of high harmonics from the plateau region of the power spectrum, in analogy with the mode-locking of a laser. In a recent study, Zhang *et al* [9] presented an efficient method to generate an isolated attosecond pulse using a two-colour laser pulse, where the harmonics between 265th and 325th order are superposed to generate an isolated ~39 as pulse with a bandwidth of 93 eV, enhancing its magnitude by three orders of magnitude over a single colour driving field.

In this section, we use harmonics from 135th to 155th order to synthesize a single attosecond pulse. We synthesize

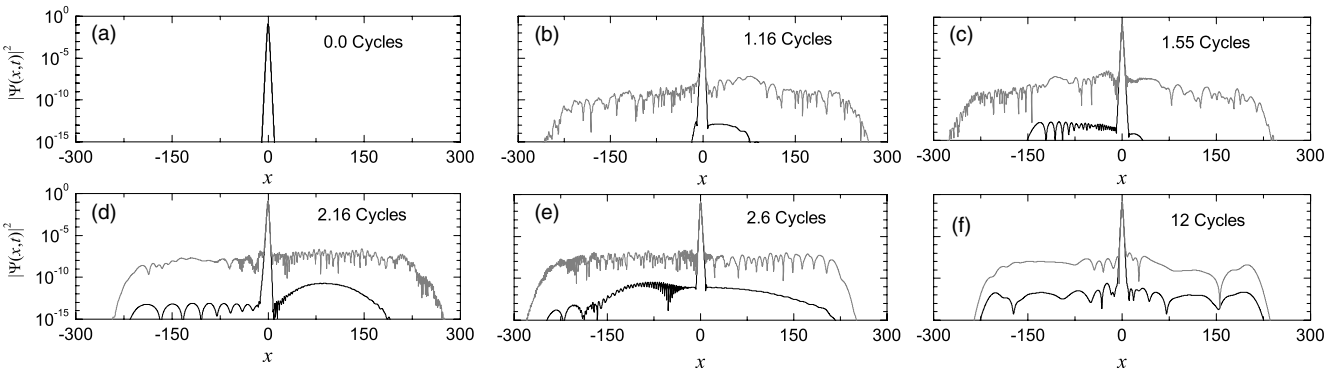


**Figure 5.** Time evolution of the spatial probability density when the atom was driven by the laser field alone (black curve), and when it is driven by the combined laser–noise field (grey curve). The laser and noise parameters are the same as those used in figure 1.

the pulse with and without noise, using the following prescription:

$$|d_F(t)|^2 = \left| \int a(\omega) F(\omega - q\omega_0) \exp(\mathrm{i}\omega t)\, \mathrm{d}\omega \right|^2, \qquad (9)$$

where $a(\omega)$ is the Fourier transform of the dipole acceleration, and $F(\omega)$ is a spectral window function defined as

$$F(\omega) = \begin{cases} 1 & -q_m\omega_0 \leqslant \omega \leqslant q_m\omega_0 \\ 0 & \text{otherwise} \end{cases}. \qquad (10)$$

Here $q_m = 10$ and $q = 145$. Setting $\phi = 0$ causes the laser field to oscillate as a sine wave, which then constitutes two equally strong intense peaks in the laser pulse under the envelope.

Figure 6 shows two equally strong peaks (black dotted curve) and the envelope (red dashed curve). The temporal profile of the attosecond pulse generated from the combined harmonics between 135th and 155th orders is shown as the solid curve, sandwiched between the two intense peaks. The attosecond pulse is composed of two partially overlapping peaks. Based on a semi-classical analysis involving quantum trajectories [22], we found that the first and incidentally the less intense peak results from emissions through the short quantum path, while the second and more intense peak results from emissions through the long quantum path. The birth (release) and termination (recombination) times of the quantum trajectories for the laser field alone are shown in figure 7 (see [22] for computational details). The pulse duration of the individual peaks in the attosecond pulse are roughly 130 as, as indicated in figure 6. Small satellite peaks on either side of the attosecond laser pulse result from the interference between the long and short electron recollision paths.

The attosecond pulse generated from the harmonics between 135th and 155th orders with the combined laser field and noise is shown in figure 8. The inset in this figure shows the synthesized pulse from high harmonics generated in the presence of noise alone, using the same window function as in figure 6. The effect of the noise on the attosecond pulse is quite noticeable in figure 8. The intensities of the attosecond pulses associated with both the short and the long quantum paths are substantially increased compared to the corresponding values in the absence of noise. Our calculations definitely show

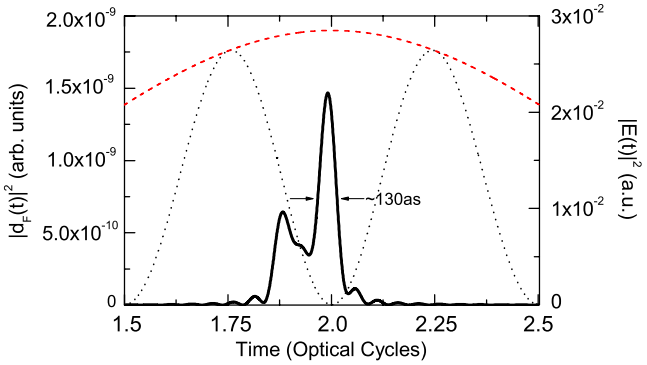


**Figure 6.** Attosecond pulse generated by superimposing the 135th through 155th harmonics generated without the noise. The laser field parameters are the same as those used in figure 1. The dotted and dashed curves represent the time profile of the driving laser field and the carrier-envelope function, respectively.

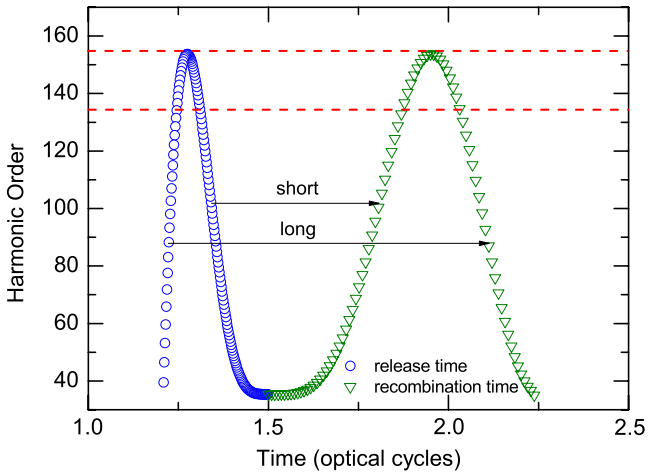


**Figure 7.** The total energy of a free electron in the laser field when it comes back to the nucleus as suggested from semi-classical analysis as a function of release and recombination time in the laser field alone. The red dashed lines mark the spectral filtering interval selected to generate an attosecond pulse.

that introducing noise to the laser field significantly increases the intensity of the attosecond pulses synthesized from the associated power spectrum. Apart from the obvious increase in the intensity of the attosecond pulse due to the enhanced harmonics in the combined laser–noise field, the first smaller

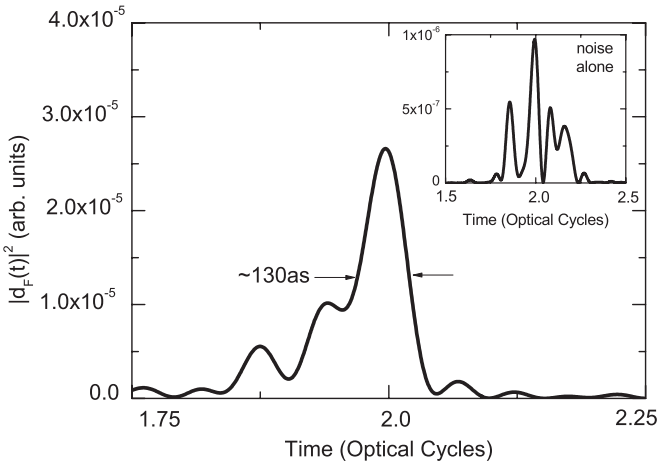


**Figure 8.** Attosecond pulse generated by superimposing the 135th up to 155th harmonics in the combined laser–noise field. The laser field parameters are the same as those in figure 1 and $\kappa/E_0 = 0.048$. The inset shows the synthesized pulse in the presence of noise alone, using the same window function.

peak in figure 6 seems to be less prominent in the pulse profile obtained from the combined laser–noise field. This suggests that the stochastic resonance induced by the addition of noise helps the long quantum path contributions become dominant.

## 5. Conclusions

We have theoretically investigated the enhancement of high harmonic yield by combining a mid-infrared laser field with a white noise. We numerically solved the one-dimensional stochastic time-dependent Shrödinger equation based on a single active electron approximation and found that the noise has nonlinear effects on the ionization probability of the atom, as reported by Singh *et al* [13, 14]. Then we also investigated how varying noise amplitudes affect the harmonic yield of the HHG spectrum. We found that roughly a factor of 45 net enhancement can be achieved in the HHG yield, using combined laser field and white noise, where the amplitude of the noise is much weaker than that of the laser field. On the other hand, we also found that for weaker noise amplitudes, the enhancement mechanism is not very sensitive to CEP. For instance, the net enhancement is negligible when $\phi = \pi/2$ compared to $\phi = 0$ for the case we studied.

Finally, we investigated attosecond pulse generation in the combined laser and noise fields. We observed that several orders of magnitude enhanced attosecond burst could be generated when the noise amplitude is set to about 1/10 of the amplitude of the driving laser field.

## Acknowledgments

IY and ZA would like to thank BAPKO of Marmara University, TR-GRID of Ulakbim and the University of Virginia for computational support. TT was supported by the Office of Basic Energy Sciences, US Department of Energy.

## References

[1] Hentschel M, Kienberger R, Spielmann Ch, Reider G A, Milosevic N, Brabec T, Corkum P B, Heinzmann U, Drescher M and Krausz F 2001 *Nature* **414** 509
[2] Wörner H J, Bertrand J B, Kartashov D V, Corkum P B and Villeneuve D M 2010 *Nature* **466** 604
[3] Itatani J, Levesque J, Zeidler D, Niikura H, Pepin H, Kieffer J C, Corkum P B and Villeneuve D M 2004 *Nature* **432** 867
[4] Corkum P 1993 *Phys. Rev. Lett.* **71** 1994
[5] Seres J, Seres E, Verhoef A J, Tempea G, Streli Ch, Wobrauschek P, Yakovlev V, Scrinzi A, Spielmann Ch and Krausz F 2005 *Nature* **433** 596
[6] Carrera J J and Chu S I 2007 *Phys. Rev.* A **75** 033807
[7] Roos L, Gaarde M B and L'Huillier A 2001 *J. Phys. B: At. Mol. Opt. Phys.* **34** 5041
[8] Ishikawa K L 2004 *Phys. Rev.* A **70** 013412
[9] Zhang G T, Wu J, Xia C L and Liu X S 2009 *Phys. Rev.* A **80** 055404
[10] Takahashi E J, Kanai T, Ishikawa K L, Nabekawa Y and Midorikawa K 2007 *Phys. Rev. Lett.* **99** 053904
[11] Wellens T, Shatokhin V and Buchleitner A 2004 *Rep. Prog. Phys.* **67** 45
[12] Benenti G, Casati G and Shepelyansky D L 1999 *Eur. Phys. J.* D **5** 311
[13] Singh K P and Rost J M 2007 *Phys. Rev.* A **76** 063403
[14] Singh K P and Rost J M 2007 *Phys. Rev. Lett.* **98** 160201
[15] Singh K P, Kenfack A and Rost J M 2008 *Phys. Rev.* A **77** 022707
[16] Weiner A M 2000 *Rev. Sci. Instrum.* **71** 1929
[17] Asnis L N, Grachev Ya V, Denisyuk I Yu and Smolyanskaya O A 2010 *J. Opt. Technol.* **77** 297
[18] Liu G-Y, Han J-L, Liu M, Teng S-Y and Cheng C-F 2010 *Chin. Phys. Lett.* **27** 067802
[19] Salieres P, L'huillier A, Antoine P and Lewenstein M 1999 *Adv. At. Mol. Opt. Phys.* **41** 83
[20] Antoine P, Gaarde M, Saliéres P, Carré B, L'Huillier and Lewenstein M 1997 *Proc. 7th Int. Conf. on Multiphoton Processes* ed P Lambropoulos and H Walther (Bristol: Institute of Physics and Physical Society) pp 142–59
[21] Agostini P and DiMauro L F 2004 *Rep. Prog. Phys.* **67** 813
[22] Ishikawa K L 2010 *Advances in Solid State Lasers Development and Applications* ed M Grishin (InTech) pp 439–64